Journal of Fluorescence (2019) 29:495–504
https://doi.org/10.1007/s10895-019-02361-9

ORIGINAL ARTICLE

Synthesis and Spectroscopic Characterization of 2-(het)Aryl Perimidine Derivatives with Enhanced Fluorescence Quantum Yields

Marco Lamperti[1] · Arianna Maria Giani[2] · Angelo Maspero[1] · Guglielmo Vesco[1] · Alessandro Cimino[1] · Roberto Negri[2] · Giovanni Battista Giovenzana[2] · Giovanni Palmisano[1] · Massimo Mella[1] · Luca Nardo[1]

Received: 19 September 2018 / Accepted: 20 February 2019 / Published online: 12 March 2019

Abstract
Perimidines are a particularly versatile family of heterocyclic compounds, whose properties are exploited in several applications ranging from industrial to medicinal chemistry. The molecular structure of perimidine incorporates a well-known efficient fluorophore, i.e.: 1,8-diaminonaphthalene. The high fluorescence quantum yield shared by most naphthalene derivatives, has enabled their use as stains for bio-imaging and biophysical characterizations. However, fluorescence is dramatically depressed in perimidine as well as in the few of its derivatives analysed so far to this respect. The use of perimidine-like molecules in life sciences might be notably fostered by enhancement of their fluorescence emission. Even more excitingly, the concomitance of both biologically active moieties and a fluorophore in the same molecular structure virtually discloses application of perimidines as drug compounds in state-of-art theranostics protocols. However, somewhat surprisingly, relatively few attempts were made until now in the direction of increasing the performances of perimidines as fluorescent dyes. In this work we present the synthesis and spectroscopic characterization of four perimidine derivatives designed to this aim, two of which result to be endowed with fluorescence quantum yields comparable to 1,8-diaminonaphthalene. A rationalization for such improved behaviour has been attempted employing TD-DFT calculations, which have unravelled the interrelations among bond structure, lone pair conjugation, local electron density changes and fluorescence quantum yield.

Keywords Perimidines · Dihydroperimidines · Fluorescence quantum yield · Theranostics

Introduction

Perimidines are heterocyclic compounds known since 1874 [1]. Their synthesis and chemical functionalization are relatively simple [2]. For this reason, they represent ideal starting compounds for an ample range of practical applications, including their exploitation in fields as diverse as industrial chemistry (as dyes, catalysts or reaction intermediates) [3, 4], biotechnology (as enzymes inhibitors) [5] and pharmacology (as antifungal, antiulcer, antibiotic and anticancer drugs) [6–10].

The perimidine (**1a** in Fig. 1) molecular structure contains 1,8-diaminonaphtalene (**1b** in Fig. 1), a high quantum yield fluorophore [11]. This feature potentially discloses the way to several additional applications in each of the above-mentioned fields and, eventually, not limited to the former. Particularly, in the biomedical context, the availability of fluorescent perimidines would have multiple repercussions ranging from nucleic acids quantification to the monitoring of biochemical reactions at the molecular level within cells or tissue, from the determination of uptake and intracellular/intra-tissue localization of this class of pharmacologically active compounds to putative applications in theranostics. An emblematic example is offered by the observation that although several perimidines exhibit very encouraging performances as chemotherapeutic agents in vitro, with IC_{50} values comparable to those of drugs routinely used in clinical practice, they are almost inactive in vivo [6]. The understanding of both the mechanisms of

Electronic supplementary material The online version of this article (https://doi.org/10.1007/s10895-019-02361-9) contains supplementary material, which is available to authorized users.

✉ Luca Nardo
luca.nardo@uninsubria.it

[1] Dipartimento di Scienza e Alta Tecnologia, Università degli Studi dell'Insubria, Via Valleggio 11, I-22100 Como, Italy

[2] Dipartimento di Scienze del Farmaco, Università degli Studi del Piemonte Orientale "A. Avogadro", Largo Donegani 2/3, I-28100 Novara, Italy

Fig. 1 Structures of the examined compounds

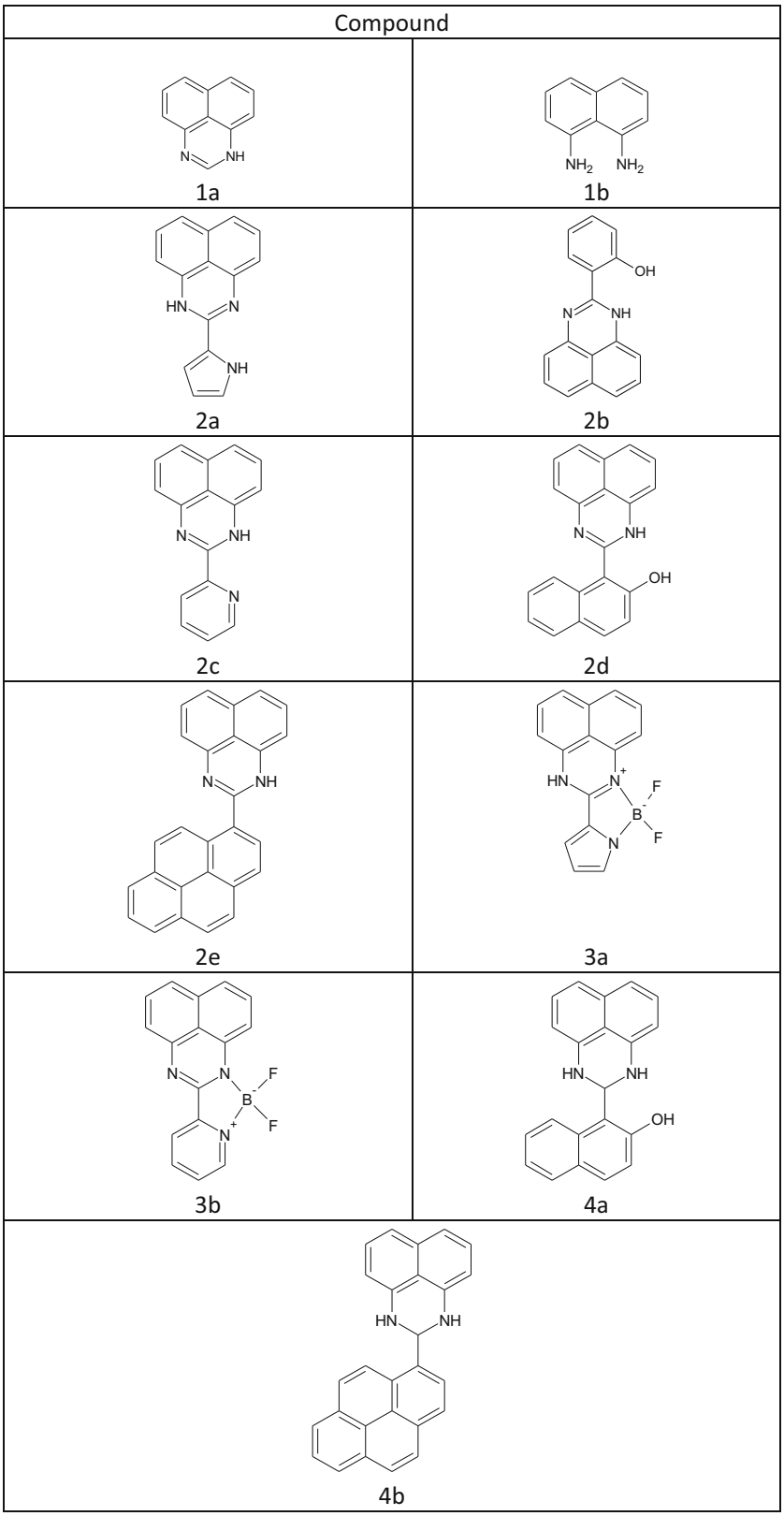

in vitro cytotoxicity and the sources of their inhibition in vivo will be notably favored by the possibility of applying to these drugs the most advanced fluorescence imaging and spectroscopy techniques, particularly those based on confocal and multi-photon excitation [12, 13]. Future developments in the design of optimized drugs based

on the perimidine structure as the active principle would be thereby valuably fostered.

Unfortunately, the *peri*-fusion of the pyrrole-nitrogens of **1b** to form the perimidine moiety results to be dramatically detrimental for the fluorescence quantum yield. According to an early report [14], this fluorescence depression seems to be related to saturation of **1b** due to an electron transfer mechanism from the unsaturated pyrrole nitrogen. Namely, *in-silico* calculations based on the Hückel molecular orbital (HMO) method show a notable electronic charge localization within the naphthalene moiety in the ground state of perimidine, which corresponds to accumulation of a residual positive charge on the C-2 of the diazine subunit. This evidence is interpreted as due to the tendency of the former moiety to withdraw the excess electron of the latter. This results in disruption of the overall aromatic character of the perimidine molecule and notably perturbs that of the naphthalene ring, thus inhibiting fluorescence. The charge transfer mechanism proposed in [14] is sketched in Scheme 1.

In a recent article [15] we have validated this hypothesis and discussed the details of the electron transfer reaction. It turned out that reducing the tendency to electron donation of the perimidine moiety to the naphthalene ring by adding suitable 2-substituents to the perimidine ring systematically induced a proportional increase in the fluorescence quantum yield. However, in the mentioned study none of the analyzed perimidine derivatives (compounds **2** in Fig. 1) exhibited satisfactory fluorescence properties, and only two compounds (**2d** and **2e** in Fig. 1) displayed sizeable fluorescence.

Harnessing the expertise matured in performing the above-described study, we have now prepared and studied four novel perimidine derivatives expressly designed to reduce at a minimum the electron transfer from the perimidine ring to the naphthalene fluorophore, with the aim of reaching fluorescence performances comparable to those of **1b**. Namely, we started from compounds **2** and, instead of acting further on the electron withdrawing character of the 2-substituent, we pursued two alternative strategies:

(i) The introduction of a BF_2 bridge to configurationally lock the nitrogen atom of either the five-membered ring of the 2-substituent of **2a** or the six-membered ring of the 2-substituent of **2c**, obtaining compounds **3a** and **3b**, respectively. The four-coordinate boron atom is commonly used to stabilize the heterocyclic structure by coordination and induce a general planarity of the overall π-system, thereby enhancing conjugation. [16]

(ii) Saturation of the diazaheterocyclic ring of the perimidine molecule in **2d** and **2e**, i.e.: relying on the corresponding 1*H*-2,3-dihydroderivatives [17] (**4a** and **4b**, respectively), in which the above mentioned electron transfer and charge accumulation on C-2 should be significantly reduced.

In this work, we present the synthesis and spectroscopic characterization of the **3**-series and **4**-series compounds, as compared to those of **1a** and **1b**. DFT calculations on the ground and excited states of these compounds are also presented in order to shed some light on the excitation dynamics and the origin of the fluorescence characteristics.

Materials and Methods

General

All chemicals of the highest purity grade were purchased from Sigma-Aldrich, Alfa Aesar or TCI Europe, and used without further purification. ^{1}H- ^{13}C- and ^{19}F-NMR were recorded on a Bruker Avance I operating at 9.4 T. Chemical shifts were reported relative to tetramethylsilane (TMS) and trichlorofluoromethane ($CFCl_3$) respectively. HR-MS were analysed on a Finnigan/thermos LTQ-FT instrument operating in the + VE mode.

Chemistry

Compound **4a-b** were prepared according to our reported procedure [15].

1-(2,3-dihydro-1H-perimidin-2-yl)-2-naphthol, (**4a**): 72%, ^{1}H-NMR δ: 10.10 (s, 1H), 9.28 (d, 1H, J = 6.4 Hz), 7.83 (t, 2H, J = 6.9 Hz), 7.38 (t, 1H, J = 8.4 Hz), 7.30 (t, 2H, J = 5.2 Hz), 7.24–7.18 (m, 3H), 7.70 (d, 2H, J = 8.4 Hz), 6.78 (s, 2H), 6.55 (d, 2H, J = 8.4 Hz), 6.32 (s, 1H). ^{13}C-NMR δ: 154.7 (C), 144.5 (C), 135.0 (C), 133.6 (C), 130.8 (CH), 129.0 (C), 128.4 (CH), 127.1 (CH), 125.8 (CH), 123.0 (CH), 118.7 (CH), 115.9 (CH), 115.7 (C), 113.1 (CH), 105.2 (CH), 61.1 (CH). HR-MS (ESI$^+$) m/z calcd for $C_{21}H_{17}N_2O^+$ $[M + H]^+$ 313.1341; found 313.1339 (Δ = -0.2 mDa).

Scheme 1 Charge transfer mechanism proposed in [14]

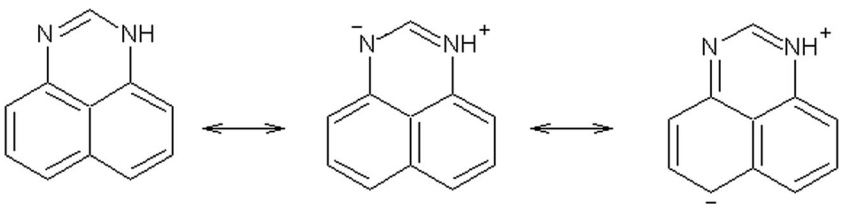

2-pyren-1-yl-2,3-dihydro-1H-perimidine, (**4b**): 65%, ^{1}H-NMR δ: 8.99 (d, 1H, J = 8.8 Hz), 8.45 (d, 1H, J = 8.1 Hz), 8.38 (d, 1H, J = 8.1 Hz), 8.34–8.31 (m, 2H), 8.23 (m, 3H,) 8.10 (t, 1H, J = 8.1 Hz), 7.26 (t, 2H, J = 8.1 Hz), 7.12 (d, 2H, J = 8.1 Hz), 7.05 (s, 2H), 6.63 (d, 2H, J = 7.3 Hz), 6.37 (s, 1H). ^{13}C-NMR δ: 144.1 (C), 135.0 (C), 134.3 (C), 131.5 (C), 131.1 (C), 130.6 (C), 129.5 (C), 123.9 (C), 121.1 (CH), 127.8 (CH), 127.5 (CH), 127.3 (CH), 126.7 (CH), 125.8 (CH), 125.7 (CH), 125.1 (CH), 124.9 (CH), 124.7 (CH), 124.4 (CH), 116.0(CH), 113.0 (C), 104 (CH), 66.1 (CH), HR-MS (ESI^{+}) m/z calcd for $C_{27}H_{19}N_2^{+}$ $[M + H]^{+}$ 371.1548; found 371.1550 (Δ = 0.2 mDa).

General Procedure for the Preparation of Compounds 3a-b

2-Arylperimidine (**2a-b**, [15] 100 mg) was dissolved in dichloromethane (30 mL). Boron trifluoride etherate (3.5 equiv) and diisopropylethylamine (3.5 equiv) were sequentially added in one portion at room temperature. The resulting reaction mixture was stirred at room temperature for 24 h. The solvent was removed by evaporation under reduced pressure, and the resulting oily mixture was separated by gravity-flow chromatography on silica-gel column (hexane/ethyl acetate, 1:1 → 3:7-gradient) affording the resulting perimidine-BF_2 adducts (**3a-b**).

*11,11-difluoro-11-bora-7,10a,11a-triaza-10a,11-dihydro-7H-pentaleno[2,-1a]phenalene, (**3a**):* 51%; ^{1}H-NMR δ: 12.72 (s, 1H) 7.37–7.29 (m, 5H), 6.94 (dq, 1H, J = 3.8, 1.0 Hz), 6.82 (d, 1 H, J = 6.9, Hz), 6.78 (dd, 1H, J = 12.7, 2.1, 6.40 (dd, 1H, J = 3.5, 2.16 Hz). ^{13}C-NMR δ: 150.3, 135.0 (C), 134.5 (C), 133.6 (C), 129.0 (CH), 128.5 (CH), 127.0 (CH), 123.9 (C), 121.8 (CH), 120.8 (CH), 119.3 (C), 115.2 (CH), 112.0 (CH), 107.9 (CH), 107.5 (CH), ^{19}F-NMR δ: −156.7 [1:1:1:1 pattern J(^{19}F-^{11}B) = 28,0 Hz], HR-MS (ESI^{+}) m/z calcd for $C_{15}H_{11}BF_2N_3^{+}$ $[M + H]^{+}$ 282.1014; found 282.1011 (Δ = -0.3 mDa).

*12,12-difluoro-12-bora-7,11a,12a-triaza-12,12a-dihydro-indeno[2,1-a]phenalene, (**3b**):* 58%, ^{1}H-NMR δ: 9.09 (d, 1H, J = 5.1 Hz), 8.66 (td, 1H, J = 7.8, 1.3 Hz), 8.41 (d, 1H, J = 8.0 Hz), 8.17 (ddd, 1H, J = 7.7, 5.5, 1.2 Hz), 7.25–7.18 (m, 3H), 7.08 (dd, 1H, J = 8.3, 1.2 Hz), 6.81 (dd, 1H, J = 6.0, 2.3 Hz), 6.50 (d, 1H, J = 10 Hz). ^{13}C-NMR δ: 150.5 (C), 146.5 (CH), 145.9 (C), 144.6 (C), 141.7 (CH), 137.7 (C), 135.8 (C), 129.3 (CH), 129.1 (CH), 128.6 (CH), 122.8 (C), 122.0 (CH), 121.5 (CH), 119.0 (CH), 115.8(CH), 104.4 (CH). ^{19}F-NMR δ: −157.8 (m), HR-MS (ESI^{+}) m/z calcd for $C_{16}H_{11}BF_2N_3^{+}$ $[M + H]^{+}$ 294.1014; found 294.1016 (Δ = 0.2mDa).

Spectroscopic Characterization

The UV-Vis absorption spectra were recorded in toluene (TOL), acetonitrile (CH_3CN), dimethylsulfoxyde (DMSO), and methanol (MeOH) by means of a Perkin Elmer Lambda 2 UV-Vis spectrophotometer. For each compound in each of the above solvents, stock solutions at 1 mM concentration were prepared by weighing the powders after storage overnight under vacuum in order to achieve desiccation. Three diluted solutions at concentration 15 μM, 20 μM, and 25 μM were prepared from each stocks, and their absorption spectra were acquired in the wavelength interval 270 nm - 650 nm (with the exception of those in TOL, were the interval was restricted to 285 nm – 650 nm due to the low transparency of the solvent in the UVB band). Fitting the plots of the absorbance values measured at the main absorption peak wavelength as a function of the nominal concentration allowed to estimate the pertaining molar extinction coefficients.

The fluorescence emission spectra were recorded by using a PTI Fluorescence Master System spectrofluorimeter. The instrument was interfaced with a dedicated acquisition software which automatically corrected the distortions of the spectral line-shape induced by wavelength-dependences in the radiance of the excitation lamp and in the quantum efficiency of the detector. Fluorescence quantum yields were determined by comparison with a solution of dimethyl-POPOP in cyclohexane ($\Phi_{Fl} = 0.93$, [18]), excited at the 343 nm absorption peak, after normalization for the relative absorbance of the samples and for the refractive index of the solvents. Subtraction of the solvent signal was performed taking advantage of the Matlab routine described in [15].

The fluorescence excitation spectra of compounds **1a**, **4a**, and **4b** were recorded in the wavelength interval 300 nm–430 nm with observation wavelength set at 500 nm for 1a and **4b**, 550 nm for **4a**.

Electronic Structure Modelling

Electronic structure calculations have been carried out using the Gaussian09 suite of codes [19]. These have involved geometry optimization at the Density Function Theory (DFT) B3LYP/LANL2DZ level, followed by Time-dependent (TD)-DFT calculations at the B3LYP/6–31++g(d,p) level to compute the excitation wavelenghts. We have limited the wavelenght window in the TD-DFT calculation as to include only the absorption lines with λ < 320 nm, which are of direct relevance for the fluorescence. Population analysis for the ground and (relevant) excited states for the studied species has been conducted with the Natural Bond Orbital (NBO) analysis [20].

Results and Discussion

The main spectroscopic parameters of perimidine, **1a**, 1,8-diaminonaphthalene, **1b**, and the novel boronated perimidines (**3a** and **3b**) and 2,3-dihydroperimidines (**4a** and **4b**) series in

Table 1 Selected spectroscopic properties of compounds **1a**, **1b**, **3a**, **3b**, **4a**, and **4b** in TOL, CH_3CN, DMSO, and MeOH: wavelength of maximum absorption, λ_{peak}, molar extinction coefficient at λ_{peak}, ε, wavelength of maximum fluorescence emission, λ_{fluo}, and fluorescence quantum yield, Φ

Compound	Solvent	λ_{peak} [nm]	ϵ [$M^{-1}cm^{-1}$]	λ_{fluo} [nm]	Φ
1a	CH_3CN	329	12,700	476	0.0013
	DMSO	333	22,900	482	0.0031
	MeOH	329	9500	485	0.0005
	TOL	331	12,400	472	0.005
1b	CH_3CN	336, 349	9100	413	0.10
	DMSO	(342), 354	13,100	411	0.30
	MeOH	334	6100	427	0.09
	TOL	320, 334	8000	403	0.13
3a	CH_3CN	333	36,800	518	0.006
	DMSO	315, 338	21,700 (@338 nm)	520	0.012
	MeOH	324, 335	35,400	533	0.0003
	TOL	341	38,100	381	0.029
3b	CH_3CN	291, 335, 350	10,100	413	0.0002
	DMSO	294, 351	19,000	498	0.0005
	MeOH	291, 348	11,700	383	0.007
	TOL	303, 339, 354	10,300	384	0.006
4a	CH_3CN	334	13,200	540	0.03
	DMSO	350	16,800	528	0.14
	MeOH	333	14,400	476	0.03
	TOL	337	18,500	468	0.33
4b	CH_3CN	341	43,800	458	0.24
	DMSO	344	49,000	420	0.08
	MeOH	340	38,500	450	0.05
	TOL	344	40,300	502	0.51

TOL, CH_3CN, DMSO, and MeOH are summarized in Table 1. First, we shortly consider the features of the absorption spectra. The peak-normalized spectral line-shapes of the different compounds dissolved in TOL, CH_3CN, DMSO, and MeOH are compared in Fig. 2, panels a), b), c), and d), respectively. A comparison of the spectra of each compound in the different solvents can be found in Supplementary Materials, Fig. S1a)-S1f). A complete discussion on the bands attribution can be found in [15]. Briefly, the UV-Vis absorption spectrum of perimidines is characterized by an intense and broad band in the UVB region, around 330–350 nm, which has been historically ascribed to a charge-transfer transition involving an electron flux from the naphthalene moiety to the perimidine peri-fused ring [14]. We tested such suggestion analysing the NBO-derived atomic charges of both the ground state (GS) and the (second) excited state (2ES) lying 327 nm above the GS; the transition to the latter is the one with the highest oscillator strength (f = 0.1035, nearly ten times higher than the second highest among the low energy transitions) and is correctly located near the experimental band maximum. Considering such state, it emerges that the transition involves two configurations, the latter deriving from the excitation from the HOMO either to the LUMO or to the orbital immediately above in energy, and displaces roughly 0.064 units of electronic charge from the NH-C=N moiety onto the naphtalene ring; the latter is already more negatively charged than the NH-C=N moiety (respectively, −1.23 versus −0.84 units of electron charge). Thus, a charge flow is indeed induced by the transition as suggested by the HMO LUMO orbital [14]; it is, however, directed oppositely to what previously proposed so that even more negative charge is injected in the naphthalene moiety. This qualitative difference is likely to be due to the intrinsic accuracy of the HMO model parameters and its inability to describe states requiring a multi-reference wave-function.

A less intense and narrower absorption peak is observed in the UVA region, at ≈250 nm, which corresponds to a π- π^* transition involving the bonding π_2 orbital of the naphthalene system as the initial state and the corresponding π_3^* antibonding orbital as the final state. Here we concentrate on the charge-transfer transition, whose features were shown in a previous article of ours [15] to be connected with the proneness of perimidine derivatives to fluoresce. Conversely, we demonstrated in [15] that, because the π- π^* transition is more local in nature, it is less affected by both environment and molecular substituents, and concomitantly less predictive of the fluorescence behaviour. As expected, all the compounds examined here display a major peak in the UVB band in any of the tested solvents (the charge-transfer band).

Interestingly, however, for compound **3b** this is not the most intense transition band, since the π-π* transition band is notably red-shifted to 290–300 nm and unusually intense, so that the charge-transfer band is reduced to either a secondary peak or a shoulder of this main peak (depending on the solvent). Note that all the other compounds considered hereby, including **3a**, show the π-π* transition peak in the usual position, i.e.: around 250 nm, in the most transparent solvents, CH_3CN and MeOH, in which the spectra were recorded in the UVA band, too (data not shown). This effect might be induced by the peculiar ionic character of the perimidine peri-fused ring in **3a**, particularly by a less π-excessive character of the naphthalene moiety as consequence of the strong electron withdrawing character of the conjugated perimidine ring. Concomitantly, the charge transfer transition occurs with an unusually high dipole strength in **3a**, which correlates with the net positive charge deposited within the peri-fused perimidine ring in the ground state due to locking with the BF_2 group (the measured molar extinction coefficients exceed 35,000 M^{-1} cm^{-1} in all solvents but DMSO).

Conversely, the same transition produces a rather faint band (i.e.: low molar extinction coefficient) in **1b**, where the peri-fused perimidine ring has been removed and the π-excessive character of the naphthalene system is lost. Intermediate values (not exceeding 20,000 M^{-1} cm^{-1}) are measured for the molar extinction coefficients of **1a** and of the boronated compound **3b**, which, although very similar to **3a**, has a neutral perimidine ring, being the electron withdrawn by the BF_2 moiety from the additional six-membered nitrogen-substituted ring. These considerations corroborate the hypotheses driven in [15] on the relationship between the proneness of the excess electron donated to the naphthalene system by the peri-fused perimidine ring to be retransferred to the latter and the intensity of the charge-transfer band. A red shift of the charge transfer band was individuated as another evidence of the excess electron proneness to be expelled from the naphthalene system in the excited state [15]. Indeed, compounds of the 3-series show transition-band peak wavelengths generally higher than those measured in the same solvents for **1a**, although not as red shifted as those detected for **1b**. The electron-donating character of the 2,3-dihydroperimidine system in the compounds of the 4-series is less predictable. However, both compounds would seem to exhibit the benchmarks of an efficient electron transfer between the 2,3-dihydroperimidine system and the naphtalene moiety in the excited state, since the charge transfer band is rather intense and red shifted. Thus, it could be inferred that the naphthalene system still conserves a π-excessive character in the ground state of these compounds, and that such excess electron population is efficiently modulated in the fluorophore

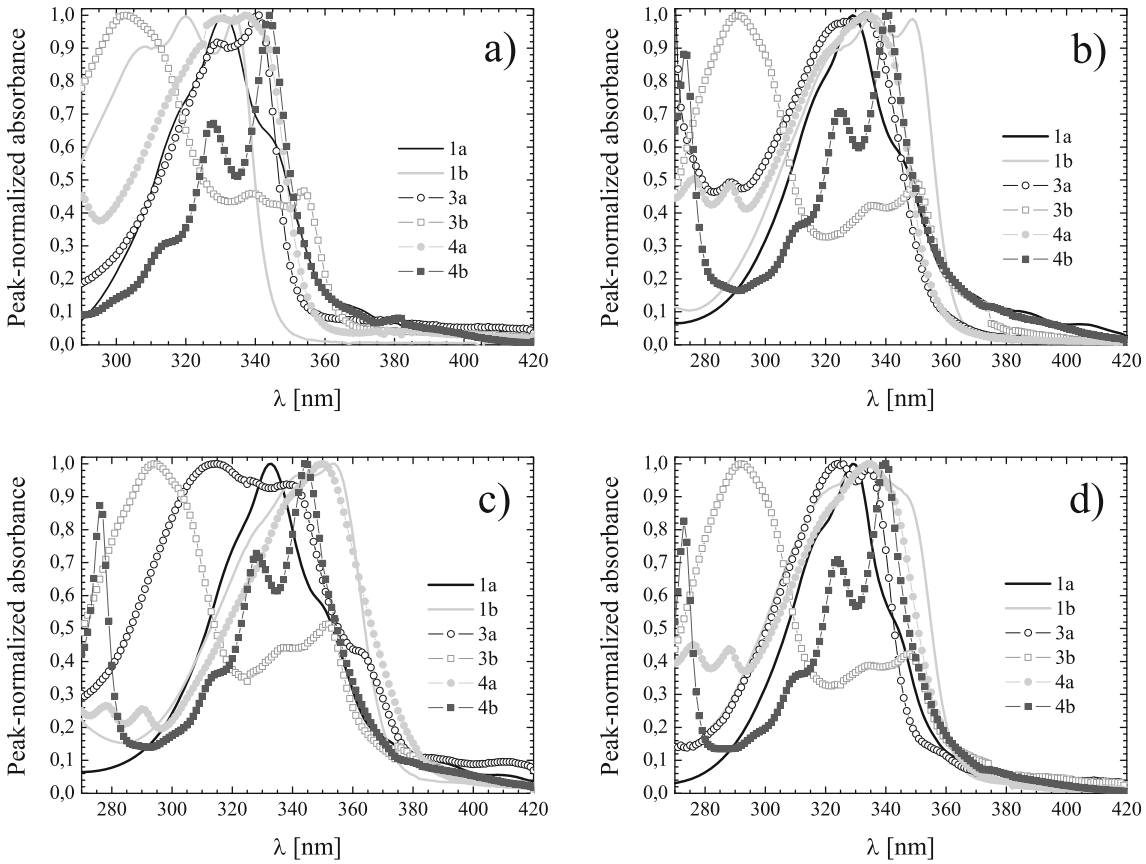

Fig. 2 Absorption spectra of **1a**, **1b**, **3a**, **3b**, **4a**, and **4b** in: a) TOL; b) CH_3CN; c) DMSO; d) MeOH

by the transition into the excited state. This is particularly evident in compound **4b**, and the highly conjugated 2-substituent of the perimidine ring was chosen with the expectation of a likely role played in favouring displacement of the excess electron on the naphthalene.

To test this idea, we computed the amount of electron density transferred upon excitation of **4a** from its GS to its (second) excited state (2ES), the latter correctly predicted to lie 333 nm above the GS and to have the highest oscillator strength (f = 0.199) among the low energy excitations by TD-DFT. De facto, 0.078 units of electron charge are, again, transferred away from the NH-C-NH moiety upon excitation, 90% of which is gathered by the naphtalene moiety of the dyhydroperimidine fragment; obviously, the difference between these two amounts is transferred onto the β-naphtolic substituent, indicating that the conjugate system of the latter is also involved in the transition defining the spectroscopic properties of **4a**. Interestingly, the amount of charge lost (0.078) by the NH-C-NH part of **4a** is 20% higher than the corresponding quantity in **1a**; this results sustain the idea proposed above of a correlation between the increase of extinction coefficients and the amount of charge transferred.

At variance with the direction of the electron displacement in **4a**, the transition of **4b** into the fourth excited state (351 nm above the GS) slightly repopulate with electrons (0.013 units of electronic charge) the NH-C-NH moiety in the dihydroperimidine fragment, 75% of the latter charge apparently coming from the naphtalenic conjugate π system (Fig. 3). Care must, however, be paid in interpreting the mentioned results, as such a small amount of charge may be very close to the limit of accuracy of the NBO approach. Notwithstanding the limited charge redistribution, the latter transition is very intense (f = 0.499) and involves both local excitation on the pyrene fragment (in particular, MO's that are only slightly modified compared to HOMO-1, HOMO, LUMO and LUMO+1 of the original pyrene) and from the global HOMO, localized on the dihydroperimidine fragment, into a π orbital distributed over the whole molecule.

We now examine the fluorescence properties of the compounds of the 3- and 4-series compared to those exhibited by the benchmark compounds **1a** and **1b**. The fluorescence emission spectra of the different compounds in TOL, CH_3CN, DMSO, and MeOH are reported in panels a), b), c), and d) of Fig. 4, respectively. In general, all the compounds emit fluorescence on a single, structure-less band peaked in the blue-green region of the spectrum, with the exception of compound **3a**, displaying a blue-shifted fluorescence peak in the violet region. The fluorescence-emission-peak wavelengths are reported in Table 1. Their relative position is not easily interpretable. Concerning the dependence, for a given compound, of the peak emission wavelength from the solvent properties, the fluorescence emission spectra of each compound in the different solvents are visually compared in Fig. S2A)-F) of the Supplementary Materials section. Compounds **1a** and **1b** are slightly affected. For compound **3b** fluorescence was very dim and did not allow a detailed characterization, while also for this chromophore the absorption spectra were slightly environment-sensitive. For the remaining three compounds, we observed notable susceptibility of the spectral features from the solvent properties. However, excluding a trivial Lippert-Mataga like dependence primarily on the solvent polarity was straightforward from our data, inasmuch as samples obtained with solvents of similar polarity produced very different spectra (see e.g. the fluorescence spectra in acetonitrile and methanol of **4a**: the latter is more than sixty nanometers blue-shifted with respect to the former). For compound **4b** an increase in polarity even produced a systematic blue-shift. To further investigate the nature of solute-solvent interactions leading to spectral changes, we performed additional characterizations of compounds **3a**, **4a**, and **4b** in another polar non-H-bonding (dichloromethane), another H-bond accepting (dimethylformamide) and another alcoholic (ethanol) solvent. The results of these experiments are included in the supplementary materials section as Figs. S3-S8. They suggest that the solvent H-bonding capabilities have major effects in dictating the spectral properties.

The fluorescence quantum yields are reported in Table 1. We begin recalling that our original working hypothesis was based on the the idea that, because the excess electron seemed to be the responsible of fluorescence quenching of the naphthalene moiety in perimidines [14], its expulsion would have provided an electronic configuration of the fluorophore in the excited state more similar to that encountered in the minimally perturbed 1,8-diaminonaphthalene. Thus, a high dipole strength of the charge transfer transition and/or a red shift of the corresponding absorption band might have been correlated with a higher fluorescence quantum yield. As fluorescence in **4a** and **4b** does not seem to be related to such mechanism (please, recall the discussion above on electronic transition-mediated charge transfer), one should consider the origin of the quantum yield results for each specific compounds.

We first consider the compounds of the 3-series, in which a modification of the naphthalene excited state has been pursued by addition of a highly electronegative BF_2 bridge connecting the unsaturated nitrogen of the perimidine ring with a nitrogen in the 2-subtituent. As discussed above, in **3b** an electron is withdrawn by the BF_2 bridge from the six-membered 2-substituent and the π-excessive character of the naphthalene moiety is only slightly affected by addition of this group. Consequently, this strategy appears inefficient. Indeed, **3b** emits fluorescence with extremely low quantum yield, which is even worse than that of **1a** in all the tested solvents but MeOH. Conversely, **3a** exhibits both a higher molar extinction coefficient and a higher fluorescence quantum yield that both **1a** and **3b** in all the solvents. However, both **3a** and **3b** have fluorescence quantum yields comparable or even somewhat

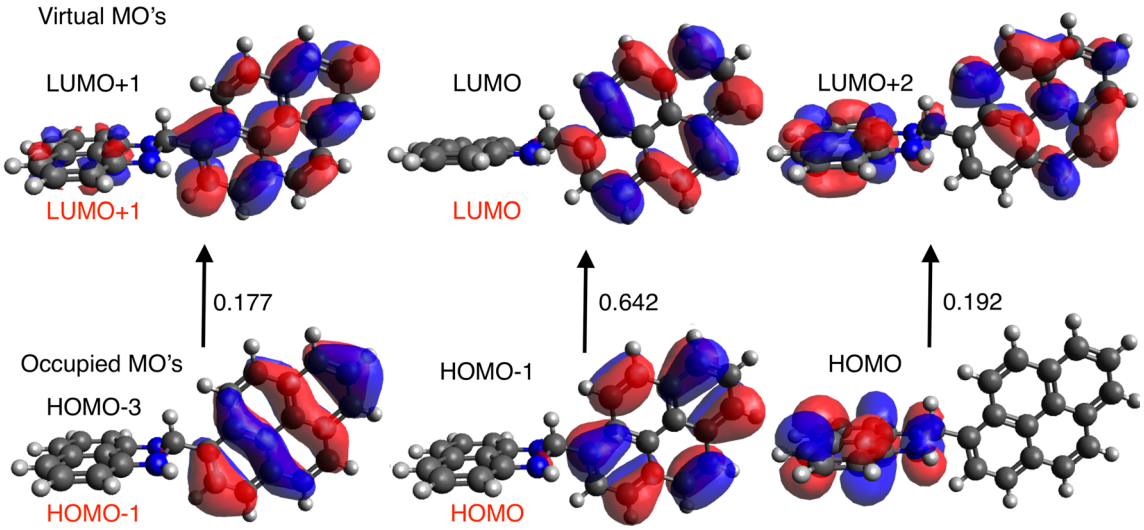

Fig. 3 Molecular orbitals involved in the intense absorption of **4b**; the numbers are the linear mixing coefficients. The location of the orbitals relative to the frontier molecular orbitals of **4b** are indicated in black; the same information for isolated pyrene is indicated in red

lower (depending on the solvent) than the corresponding non-boronated compounds in the 2-series (see [15] for details). This suggests that in **3a**, although modification of the excited state electron density is actually pursued by the introduction of the BF_2 group, this substitution seems to induce other means of fluorescence quenching.

The second strategy adopted to reduce the π-excessive nature of the naphthalene system in perimidine-like structures, i.e.: saturation of the perimidine ring, proved, in principle, to be more effective. Indeed, both compounds of the 4-series exhibit high molar extinction coefficients and red-shifted absorption in the charge transfer band, all of which are well

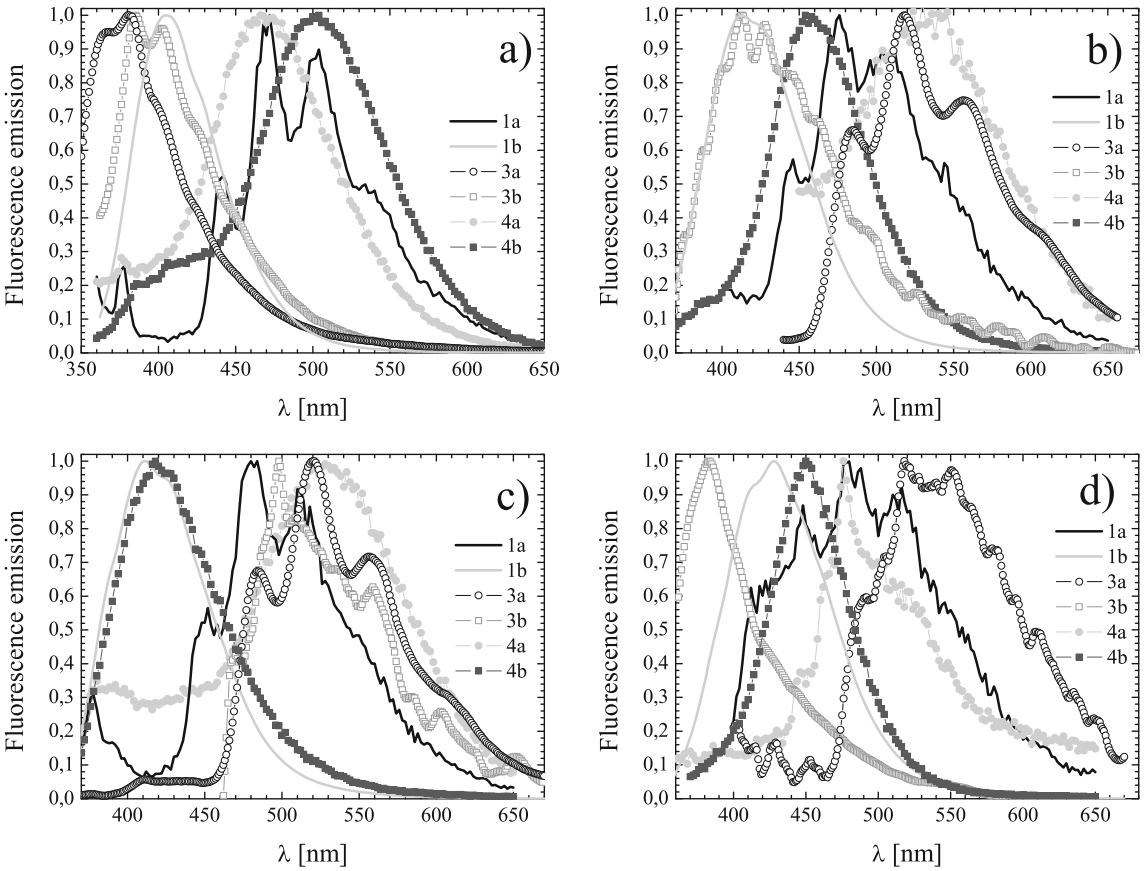

Fig. 4 Fluorescence emission spectra of **1a**, **1b**, **3a**, **3b**, **4a**, and **4b** in a) TOL; b) CH_3CN; c) DMSO; d) MeOH

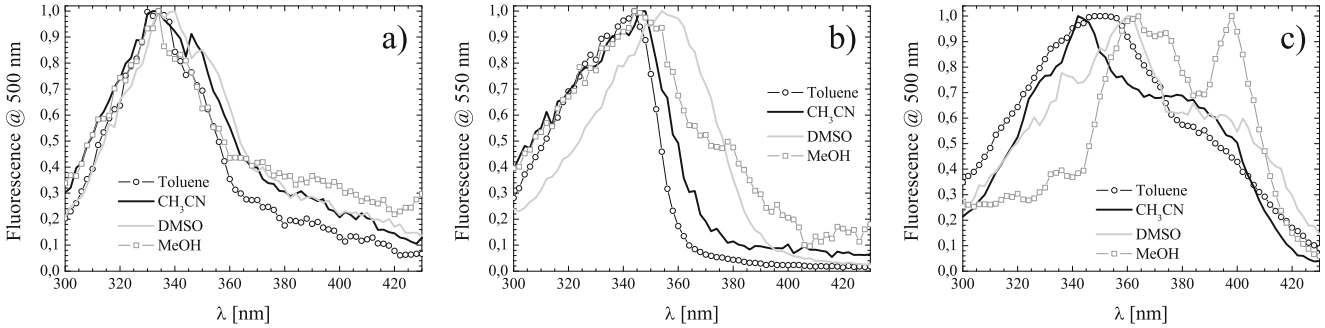

Fig. 5 Excitation spectra of compounds **1a**, panel (**a**); **4a**, panel (**b**); and **4b**, panel (**c**); in TOL (circles), CH_3CN (black line), DMSO (gray line), and MeOH (squares)

reproduced by the TD-DFT results. These finding, however, appear to be related to either more charge being injected onto the naphthalene moiety of perimidine (in **4a**) or the substantial involvement of the pyrene pendant (in **4b**, see the discussion above). Despite this, and of high interest for our overall goal, these compounds are also endowed with fluorescence quantum yields comparable or even somewhat higher than those of **1b** in all the tested solvents. It should be noted that, while the enhancement in conjugation provided by addition of polyaromatic rings as 2-substituents seems to have beneficial effects on the fluorescence quantum yield, of both **4a** and **4b** in inert environment (TOL), polarity effects and/or putative H-bonding interactions with solvent molecules seem to exist and to lead to detrimental effects. An explanation for this phenomenon can be attempted in the case of **4a**, whose dinuclear 2-substituent is hydroxylated. Indeed, both in the corresponding non-hydrogenated compound **2d** and in compound **2b**, 2-hydroxyphenyl-1*H*-perimidine, the same behaviour has been observed. In case of **2b** the decay photophysics was elucidated by Catalán and coworkers as early as in 1996, and the role of the hydroxyl moiety in solute-solvent interactions and in fluorescence depression was highlighted [21].

In order to investigate further the fluorescence properties of the compounds of the 4-series, excitation spectra of **4a** and **4b** were recorded in all the solvents. In Fig. 5 they are compared with those of **1a**. While the excitation spectra in all the solvents are essentially superimposed to the corresponding absorption spectra for **1a** and only slightly red-shifted with respect to the corresponding absorption spectra for **4a**, examination of **4b** has revealed significant differences between absorption and excitation line-shapes, suggesting a non-trivial excited-state dynamics for the latter compound. In particular, while the distinction of two peaks at 330 nm and 350 nm within the major absorption band is no more apparent in the excitation spectra, excitation results very efficient at 380 nm, in correspondence to what appears a rather low-intensity shoulder in absorption. In principle, the dynamics suggested by the long wavelength shoulder or peak in the excitation spectrum for **4b** may be justified by the involvement of the pyrene π system in the excitation. For instance, the difference between the eigenvalues of the pyrene-localized HOMO and LUMO suggest an absorption resonance around 334 nm, which, following nuclear dynamics, may luminesce al longer wavelengths.

Conclusions

In this article, taking advantage of our previous studies on the photophysics of perimidine derivatives, we synthesized novel perimidine-based compounds with the aim of endowing them with fluorescence properties comparable to those of the high-quantum-yield fluorophore naphthalene, which is contained within the perimidine structure. Our attempts were devoted to reduce the tendency of the naphthalene system to acquire a π-excessive character in the perimidines excited state. We pursued this goal by adopting two different strategies: (i) locking the perimidine and substituent ring of two previously synthesized 2-substituted perimidine derivatives with a BF_2 moiety; and (ii) saturating the perimidine ring to the corresponding 2,3-dihydroderivatives. The second strategy demonstrated superior efficacy in enhancing the fluorescence properties, albeit due to causes deviating from what originally thought. Nevertheless, it yielded perimidines with fluorescence quantum yields comparable to those of naphthalene.

Funding This research did not receive any specific grant from funding agencies in the public, commercial, or not-for-profit sectors.

Compliance with Ethical Standards

Conflict of Interest The authors declare that they have no conflict of interest.

References

1. de Aguiar A (1874) Ueber einige Abkömmlinge des α- und β-Diamidonaphtalins. Ber Dtsch Chem Ges 7:309–319
2. Pozharskii AF, Dal'nikovkaya VV (1981) Perimidines. Russ Chem Rev 50:816–835

3. Undheim K, Benneche C (1996) Pyrimidines and their benzo-derivatives. In: Katritzky AR, Rees CW, Scriven EFV (Eds) Comprehensive heterocyclic chemistry Pergamon, Oxford, Vol. 6, pp. 93–231
4. Bazinet P, Yap GPA, Richeson DS (2003) Constructing a stable carbine with a novel topology and electronic framework. J Am Chem Soc 125:13314–13315
5. Wang W-L, Yang D-L, Gao L-X, Tang C-L, Ma W-P, Ye H-H, Zhang S-Q, Zhao Y-N, Xu H-J, Hu Z, Chen X, Fan W-H, Chen H-J, Li J-Y, Nan F-J, Li J, Feng B (2014) 1*H*-2,3-Dihydroperimidine derivatives: a new class of potent protein tyrosine phosphatase 1B inhibitors. Molecules 19:102–121
6. Herbert JM, Woodgate PD, Denny WA (1987) Potential antitumor agents. 53. Synthesis, DNA binding properties, and biological activity of perimidines designed as "minimal" DNA intercalating agents. J Med Chem 30:2081–2086
7. Bu X, Deady LW, Finlay GJ, Baguley BC, Denny WA (2001) Synthesis and cytotoxic activity of 7-oxo-7H-dibenz[f, Ij]isoquinoline and 7-oxo-7H-benzo[e]perimidine derivatives. J med Chem 44:2004-2014, and ref. In: therein
8. Starshikoy NM, Pozharskii FT (1973) Synthesis of 2-(5-halogeno-2-furyl)-2,3-dihydroperimidines. Chem Heterocycl Compd 9:922–924
9. Azeez HJ, Salih KM (2014) Synthesis, characterization and biological activity of 2-aryl −2,3-dihydro-1-H-perimidine. Res Pharmaceut Biotech 3:1–6, and refs. therein
10. Farghaly TA, Mahmoud HK (2013) Synthesis, tautomeric structures, and antitumor activity of new perimidines. Arch Pharm Chem Life Sci 346:392–402
11. Schwarz FP, Wasik SP (1976) Fluorescence measurements of benzene, naphthalene, anthracene, pyrene, fluoranthene, and benzo[e]pyrene in water. Anal Chem 48:524–528
12. Gregori M, Bertani D, Cazzaniga E, Orlando A, Mauri M, Bianchi A, Re F, Sesana S, Minniti S, Francolini M, Cagnotto A, Salmona M, Nardo L, Salerno D, Mantegazza F, Masserini M, Simonutti R (2015) Investigation of functionalized poly(*N*,*N*-dimethylacrylamide)-*block*-polystyrene nanoparticles as novel drug delivery system to overcome the blood–brain barrier in vitro. Macromol Biosci 15:1687–1697
13. Abbotto A, Baldini G, Beverina L, Chirico G, Collini M, D'Alfonso L, Diaspro A, Magrassi R, Nardo L, Pagani GA (2005) Dimethyl-pepep: a DNA probe in two-photon excitation cellular imaging. Biophys Chem 114:35–41
14. Minkin VI, Zhdanov YA, Sadekov ID, Raevskii OA, Garnovskii AD (1967) Structure and properties of perimidine and its derivatives. Chem Heterocycl Compd 3:855–860
15. Giani A, Lamperti M, Maspero A, Cimino A, Negri R, Giovenzana G, Palmisano G, Nardo L (2016) Fluorescence studies on 2-(het)aryl perimidine derivatives. J Lumin 179:384–392
16. Frath D, Massue J, Ulrich G, Ziessel R (2014) Luminescent materials: locking π-conjugated and heterocyclic ligands with boron(III). Angew Chem Int Ed 53:2290–2310
17. Varsha G, Arun A, Robinson PP, Sebastian M, Varghese D, Leeju P, Jayachandran VP, Yusuff KKM (2010) Two new fluorescent heterocyclic perimidines: first syntheses, crystal structure, and spectral characterization. Tetrahedron Lett 51:2174–2177
18. Berlman IB (1971) Handbook of fluorescence spectra of aromatic molecules. Academic Press, N.Y
19. M. J. Frisch et al. *Gaussian 09* (Gaussian, Inc., Wallingford CT, 2009)
20. Foster JP, Weinhold F (1980) Natural hybrid orbitals. J Am Chem Soc 102:7211–7218
21. Catalan J, del Valle JC, Claramunt RM, Sanz D, Dotor J (1996) Photophysics of the 2-(2′-hydroxyphenyl)perimidine: on the fluorescence of the enol form. J Lumin 68:165–170